Electronic Supplementary Information (ESI) for

Dual-Photofunctional Organogermanium Compound Based on Donor–Acceptor–Donor Architecture

Alexandra Nyga,[a†] *Takahito Kaihara,*[b†] *Takumi Hosono,*[b] *Massimiliano Sipala,*[a] *Patrycja Stachelek,*[c] *Norimitsu Tohnai,*[b] *Satoshi Minakata,*[b] *Leonardo Evaristo de Sousa,*[d] *Piotr de Silva,*[d*] *Przemyslaw Data,*[a*] *and Youhei Takeda*[b*]

[a]Faculty of Chemistry, Silesian University of Technology, M. Strzody 9, 44-100 Gliwice, Poland
[b]Department of Applied Chemistry, Graduate School of Engineering, Osaka University, Yamadaoka 2-1, Suita, Osaka 565-0871, Japan
[c]Chemistry Department, Durham University, South Road, Durham DH1 3LE, United Kingdom
[d]Department of Energy Conversion and Storage, Technical University of Denmark, Anker Engelunds Vej 301, 2800 Kongens Lyngby, Denmark
[†]These authors contributed equally to this work.

e-mail: pdes@dtu.dk; przemyslaw.data@polsl.pl; takeda@chem.eng.osaka-u.ac.jp

Table of Contents

General Remarks. All reactions were carried out under an atmosphere of nitrogen unless otherwise noted. Melting points were determined on a Stanford Research Systems MPA100 OptiMelt Automated Melting Point System. ^{1}H and ^{13}C spectra were recorded on a JEOL JMTC-400/54/SS Spectrometer (^{1}H NMR, 400 MHz; ^{13}C NMR, 100 MHz) using tetramethylsilane as an internal standard ($\delta = 0$ ppm). Infrared spectra were acquired on a SHIMADZU IRAffinity-1 FT-IR Spectrometer. Mass spectra and High-resolution mass spectra were obtained on a JEOL JMS-700 Mass Spectrometer. Products were purified by chromatography on silica gel BW-300 and Chromatorex NH (Fuji Silysia Chemical Ltd.). Analytical thin-layer chromatography (TLC) was performed on pre-coated silica gel glass plates (Merck silica gel 60 F254 and Fuji Silysia Chromatorex NH, 0.25 mm thickness). Compounds were visualized with UV lamp.

Materials. 3,11-dibromodibenzo[*a,j*]phenazine (**5**) [CAS No. 1620543-64-7] was prepared according to the reported procedure.[S1] 2-Bromo-*N*-(2-bromophenyl)-*N*-(4-methoxybenzyl)aniline (**2**) [CAS No. 1525711-66-3] was prepared according to the procedures in literature.[S2] Commercial reagents were purchased (Sigma-Aldrich, TCI, or FUJIFILM Wako Pure Chemical Corp.) and used as received.

Photophysics. UV-vis spectra were recorded on a Shimadzu UV-2550 spectrophotometer. Steady-state emission spectra were recorded on a HAMAMATSU C11347-01 spectrometer with an integrating sphere and Jobin Yvon Horiba Fluorolog 3, with solvent studies performed in clean 1 cm path-length photoluminescence cuvettes (Arieka Cells) and temperature dependent film photoluminescence films studies performed on within a liquid N_2 cooled cryostat (Janis Research). Photoluminescence spectra were calibrated for detector efficiency using company supplied, instrument specific calibration files. The emitter materials was also degassed in toluene solvent using a custom made 1 cm path-length degassed cell stoppered with a Young tap and degassed using 5 freeze/thaw/pump cycles. The photoluminescence quantum yield (PLQY) of emitters in toluene solvent was determined using the reference method against 9,10-diphenylanthracene (DPA). Solid-state samples were prepared as 1% w/w ratio emitters in Zeonex® polymer host on clean/dry sapphire disc substrates. Phosphorescence, prompt fluorescence (PF), and delayed fluorescence (DF) spectra and decays were recorded using nanosecond gated luminescence and lifetime measurements (from 400 ps to 1 s) using either third harmonics of a high energy pulsed DPSS laser emitting at 355 nm (Q-Spark A50-TH-RE). Emission was focused onto a spectrograph and detected on a sensitive gated iCCD camera (Stanford Computer Optics) having a sub-nanosecond resolution. PF/DF time-resolved measurements were performed by exponentially increasing gate and integration times. Temperature-dependent experiments were conducted using an helium cryostat (Janis Research) under a vacuum.

Devices. NPB (*N*,*N*′-di(1-naphthyl)-*N*,*N*′-diphenyl-(1,1′-biphenyl)-4,4′-diamine) was used as a Hole Injection Layer (HIL) and Hole Transport Layer (HTL), TSBPA (4,4'-(Diphenylsilanediyl)bis(N,Ndiphenylaniline)) and TAPC (4,4′-Cyclohexylidenebis[*N*,*N*-bis(4-methylphenyl)benzenamine]) were used as a Electron Blocking Layer (EBL). TPBi 2,2',2"-(1,3,5-Benzinetriyl)-tris(1-phenyl-1-H-benzimidazole) was introduced as an Electron Transport Layer (ETL). Lithium fluoride (LiF) and aluminium were used as the cathode. Organic semiconductors and aluminium were deposited at a rate of 1 Ås-1, and the LiF layer was deposited at 0.1 Ås-1. TCTA (Tris(4-carbazoyl-9-ylphenyl)amine) and CBP 4,4′-bis(*N*-carbazolyl)-1,1′-biphenyl, were used as hosts for all emitters. All materials were purchased from Sigma Aldrich or Lumtec and were purified by temperature-gradient sublimation in a vacuum. OLEDs have been fabricated on pre-cleaned, patterned indium-tin-oxide (ITO) coated glass substrates with a sheet resistance of 20 Ω/sq and ITO thickness of 100 nm. All small molecules and cathode layers were thermally evaporated in a Kurt J. Lesker SuperSpectros 200 evaporation system under pressure of 10^{-7} mbar without breaking the vacuum. The sizes of pixels were 4 mm^2, 8 mm^2 and 16 mm^2. Each emitting layer has been formed by co-deposition of dopant and host at the specific rate to obtain 10% content of the emitter. The characteristics of the devices were recorded using a 6-inch integrating sphere (Labsphere) inside the glovebox connected to a Source Meter Unit and Ocean Optics USB4000 spectrometer.

Electrochemistry. The electrochemical investigation was carried out using potentiostats Autolab PGSTAT20 and Biologic SP150 system. Cyclic voltammetric measurements were conducted with 1 mM concentration of **1** with 0.1 M BF_4 in DCM, at room temperature and 50 mV/s potential rate, calibrated against the ferrocene/ferrocenium (Fc/Fc^+) redox couple. The electrochemical cell comprised a 1 mm diameter platinum (Pt) disk as working electrode (WE), Ag/AgCl electrode as reference electrode (RE) and platinum coil as an auxiliary electrode (AE).

Synthetic Procedures and Spectroscopic Data of New Compounds.

Synthetic procedures for 10,10-diphenyl-5,10-dihydrodibenzo[b,e][1,4]azagermine (**4**) [CAS No. 2283363-50-6]

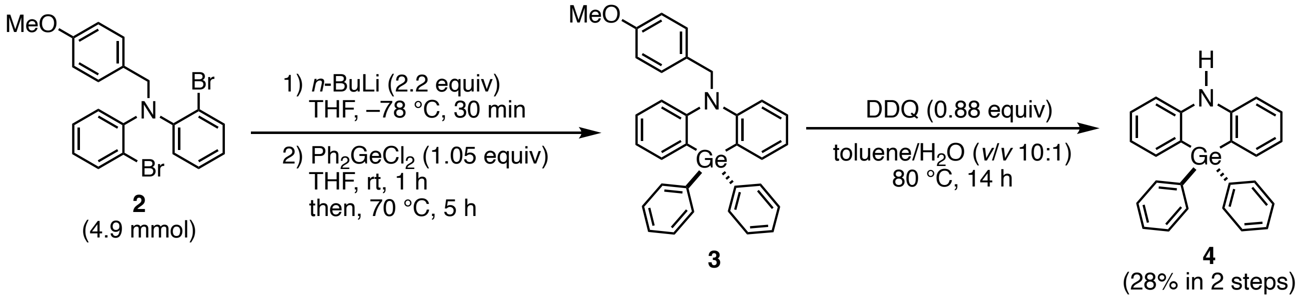

The 200 mL three-necked round-bottomed flask equipped with a magnetic stirring bar, a three-way cock, and two septum was flame-dried under vacuum and refilled with an N$_2$ atmosphere. To the flask, were added 2-bromo-*N*-(2-bromophenyl)-*N*-(4-methoxybenzyl)aniline (2.2 g, 4.9 mmol, 1.0 equiv) and THF (30 mL). The flask was cooled to –78 °C, and *n*-BuLi [6.9 mL, 11.0 mmol, 1.6 M (*n*-hexane solution), 2.2 equiv] was added dropwise to the solution over 10 min. The reaction mixture was stirred at –78 °C for 30 min, and diphenyldichlorogermane (1.1 mL, 1.65 g, 5.25 mmol, 1.05 equiv) was added to it dropwise. The flask was removed from the cooling bath, allowed to warm up to room temperature and stirred for 30 min. The reaction mixture was then heated up to 70 °C and stirred for 5 h. The reaction mixture was allowed to cool to room temperature and quenched with water. The organic layer was extracted with ethyl acetate (30 mL × 3) and dried over Na$_2$SO$_4$, which was then dried by evaporating organic solvents under reduced pressure to give crude product (2.7 g). The crude product was purified by flash column chromatography on an NH silica gel (eluent: *n*-hexane:EtOAc = 100:0 to 95:5) to provide 5-(4-methoxybenzyl)-10,10-diphenyl-5,10-dihydrodibenzo[*b*,*e*][1,4]azagermine as white solid (2.0 g). *R*$_f$ 0.68 (*n*–hexane:EtOAc = 8:2). This intermediate was subsequently subjected to the next reaction without further purification.

To a 50 mL two-necked round-bottomed flask equipped with a magnetic stirring bar, a three-way cock, and a septum, were added 5-(4-methoxybenzyl)-10,10-diphenyl-5,10-dihydrodibenzo[*b*,*e*][1,4]azagermine (1.29 g, 2.5 mmol, 1.0 equiv) and DDQ (0.5 g, 2.2 mmol, 0.88 equiv). The flask was evacuated and replaced with N$_2$ gas for three times. To the flask, toluene (10 mL) and distilled water (1 mL) were added. The mixture was stirred at 80 °C for 14 h. The reaction mixture was allowed to cool to room temperature and extracted with ethyl acetate (10 mL× 3), which was then evaporated to give the crude product (1.78 g). The crude product was purified by flash chromatography on an NH silica gel (eluent: *n*-hexane:EtOAc = 8:2) to give the title compound as white solid (0.35 g, 0.89 mmol, 28% in 2 steps). Mp 199 °C (dec.); *R*$_f$ 0.30 (*n*-hexane:EtOAc 8:2, NH silica); ^{1}H NMR (400 MHz, CDCl$_3$): δ 7.56–7.54 (m, 4H), 7.50 (dd, *J* = 7.6, 1.2 Hz, 2H), 7.36–7.28 (m, 8H), 6.92 (dd, *J* = 7.2, 7.2 Hz, 2H), 6.83 (d, *J* = 8.4 Hz, 2H), 6.51 (brs, 1H); ^{13}C NMR (100 MHz, CDCl$_3$): δ 145.9, 136.9, 135.7, 134.9, 130.3, 129.1, 128.3, 120.1, 115.6, 115.4; IR (ATR): ν 3398, 3064, 3047, 3026, 1597, 1573, 1514, 1483, 1456, 1433, 1336, 1236, 1219, 1163, 1091, 1070, 1033, 1026, 893, 881, 754, 734 cm^{-1}; MS (EI$^+$): *m/z* (relative intensity, %) 395 ([M]$^+$, 62), 393([M–2]$^+$, 44), 391 ([M–4]$^+$, 32), 318 ([M–Ph]$^+$, 100), 316 ([M–2–Ph]$^+$, 79), 314 ([M–4–Ph]$^+$, 57), 241 ([M–2Ph]$^+$, 7), 167 ([M–Ge–2Ph]$^+$, 29); HRMS (EI$^+$): *m/z* calcd for $C_{24}H_{19}GeN$ (M) 395.0729, found 395.0731.

Synthetic procedures for 3,11-bis(10,10-diphenyldibenzo[b,e][1,4]azagermin-5(10H)-yl)dibenzo[a,j]phenazine (**1**)

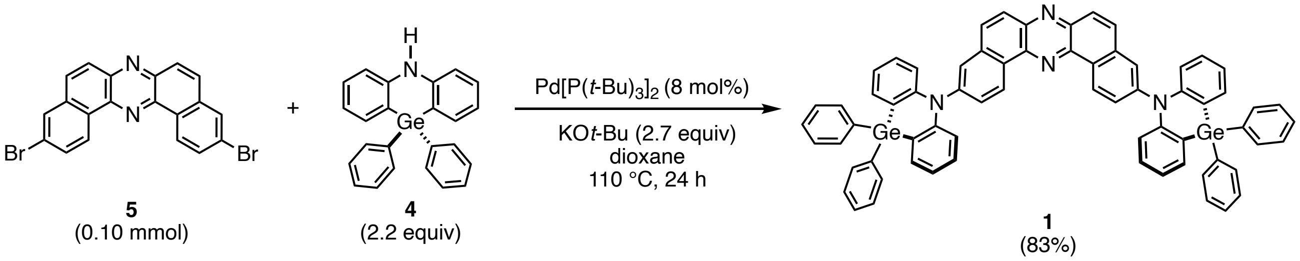

To a two-necked reaction tube (10 mL) equipped with a magnetic stir bar, were added 3,11-dibromo-dibenzo[*a,j*]phenazine (**5**) (44.0 mg, 0.10 mmol, 1.0 equiv) and 10,10-diphenyl-5,10-dihydrodibenzo[*b,e*][1,4]azagermine (**4**) (85.0 mg, 0.22 mmol, 2.2 equiv). The tube was transferred into a glove box. To the tube, were added Pd[P(*t*-Bu)$_3$]$_2$ (3.9 mg, 7.6 μmol, 8 mol%) and KO*t*-Bu (30 mg, 0.27 mmol, 2.7 equiv). The tube was sealed with a rubber septum and taken out of the glove box. 1,4-Dioxane (4 mL) was added to the tube under a stream of N_2 gas at room temperature, and the resulting mixture was stirred at 110 °C for 24 h. Water (15 mL) was added to the reaction mixture, and the organic layer was extracted with CH_2Cl_2 (20 mL × 3). The combined organic extracts were dried over Na_2SO_4, and the solvent was evaporated in vacuo to give the crude product, which was purified by flash column chromatography on NH silica gel (eluent: *n*-hexane/$CHCl_3$ 8:2) followed by recrystallization from a two-phase solvent of *n*-hexane/$CHCl_3$, affording the title compound **1** as yellow solid (88.6 mg, 0.08 mmol, 83%). Mp > 400 °C (dec.); T_d (5 wt% loss) = 466 °C (under N_2); 431 °C (under air); R_f 0.25 (*n*-hexane:EtOAc 8:2, NH silica); ^{1}H NMR (400 MHz, $CDCl_3$): δ 9.71 (d, J = 8.8 Hz, 2H), 8.10 (d, J = 9.2 Hz, 2H), 8.00 (d, J = 9.2 Hz, 2H), 7.76 (d, J = 2.0 Hz, 2H), 7.72 (dd, J = 8.8, 2.0 Hz, 2H), 7.62–7.58 (m, 12H), 7.38–7.36 (m, 12H), 7.22 (ddd, J = 9.6, 6.2, 1.6 Hz, 4H), 7.04 (ddd, J = 7.4, 6.8, 1.2 Hz, 4H), 6.80 (d, J = 8.4 Hz, 4H); ^{13}C NMR (100 MHz, $CDCl_3$): δ 149.3, 145.9, 142.7, 140.6, 135.8, 135.6, 135.3, 135.1, 132.2, 129.9, 129.3, 129.1, 128.3, 128.0, 127. 7, 127.6, 126.3, 122.5, 121.7, 120.3; IR (ATR): ν 3064, 1587, 1552, 1477, 1452, 1431, 1352, 1300, 1242, 1180, 1161, 1089, 995, 927, 856, 798, 748, 734 cm^{-1}; MS (FAB$^+$, NBA): *m/z* (relative intensity, %) 1065 ([M+H]$^+$, 19), 1064 (M$^+$, 19), 987 ([M–Ph]$^+$, 10); HRMS (FAB$^+$, NBA): *m/z* calcd for $C_{68}H_{46}Ge_2N_4$ (M) 1064.2155, found 1064.2220. Anal. Calcd for $C_{68}H_{46}N_4Ge_2$: C, 76.73; H, 4.36; N, 5.26. Found: C, 77.02; H, 4.30; N, 5.33.

Single Crystal X-Ray Crystallographic Analysis.

Crystallographic analysis of compound **4**: The single crystal suitable for the X-ray crystallographic analysis was grown from a biphasic solution of *n*-hexane/$CHCl_3$ by slow evaporation. XtaLAB P200 diffractometer with graphite monochromated CuKα radiation (λ = 1.54187 Å) to a $2\theta_{max}$ value of 148.9° at 213 K. The cell refinements were performed with a software CrysAlisPro 1.171.39.20a.[S3] The crystal structure was solved by direct methods (SHELXT Version 2014/5).[S4] All calculations were performed with the observed reflections [I > 2σ(I)] with the program CrystalStructure crystallographic software packages,[S5] except for refinement which was performed by SHELXL.[S6] The non-hydrogen atoms were refined anisotropically, and hydrogen atoms were refined using the riding model. The crystal data are summarized in Table SX. CCDC-2153796 contains the supplementary crystallographic data for **4**, which are available free of charge from the Cambridge Crystallographic Data Center (CCDC) via www.ccdc.cam.ac.uk/data_request/cif.

Table S1. Summary of the crystallographic data of compound **4**.

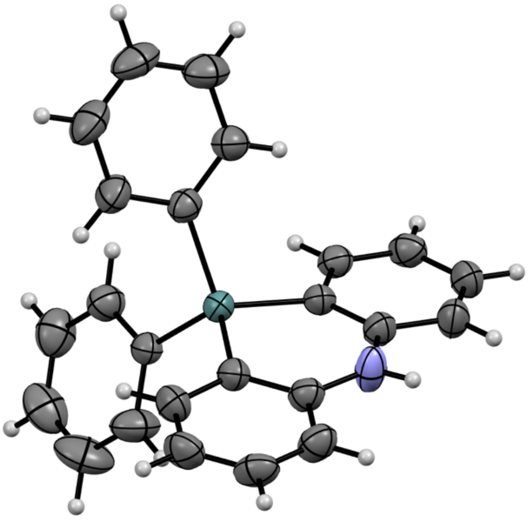

Empirical Formula	$C_{24}H_{19}GeN$	
Formula Weight	394.01	
Crystal System	monoclinic	
Space Group	$P2_1/c$ (#14)	
Unit cell dimensions	a = 10.89970(13) Å	α = 90°
	b = 8.57542(10) Å	β = 92.5617(10)°
	c = 20.1183(2) Å	γ = 90°
V	1878.57(4) Å^3	
Z	4	
Density (calculated)	1.393 g/cm^3	
Absorption coefficient	22.417 cm^{-1}	
R_1 [I>2σ(I)]	0.0322	
wR_2 (all data)	0.0932	
Crystal size	0.200 × 0.100 × 0.100 mm	
Goodness-of-fit on F^2	1.064	
Reflections collected/unique	9935/3720 [R(int) = 0.0264]	

Cyclic Voltammetry

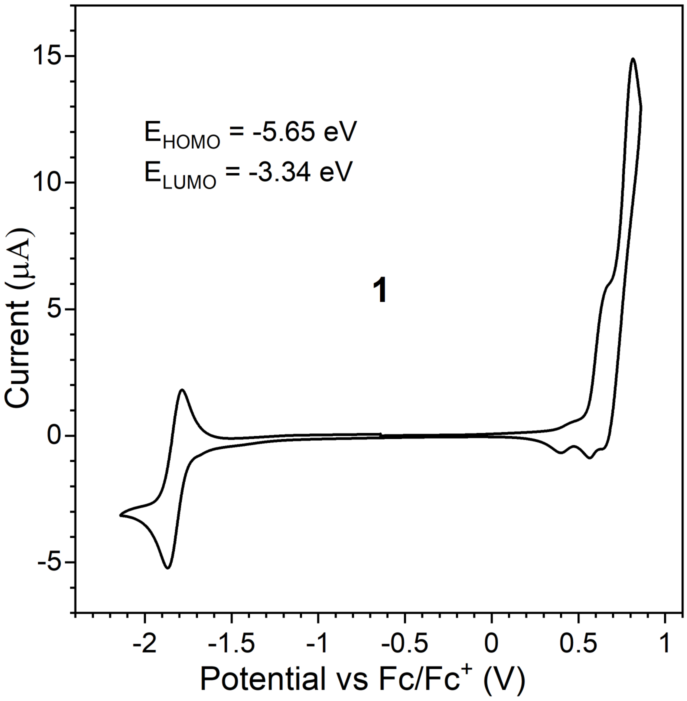

Fig. S1 Cyclic voltammogram of **1** (1 mM) in DCM Bu_4NBF_4 (0.1 M) electrolyte.

Thermogravimetric Analysis (TGA)

The TGA profiles of **1** were obtained using a Pt pan under the air or the N_2 gas flow (200 mL/min), starting from 40 °C to 1000 °C at the ramp rate of 10 °C/min.

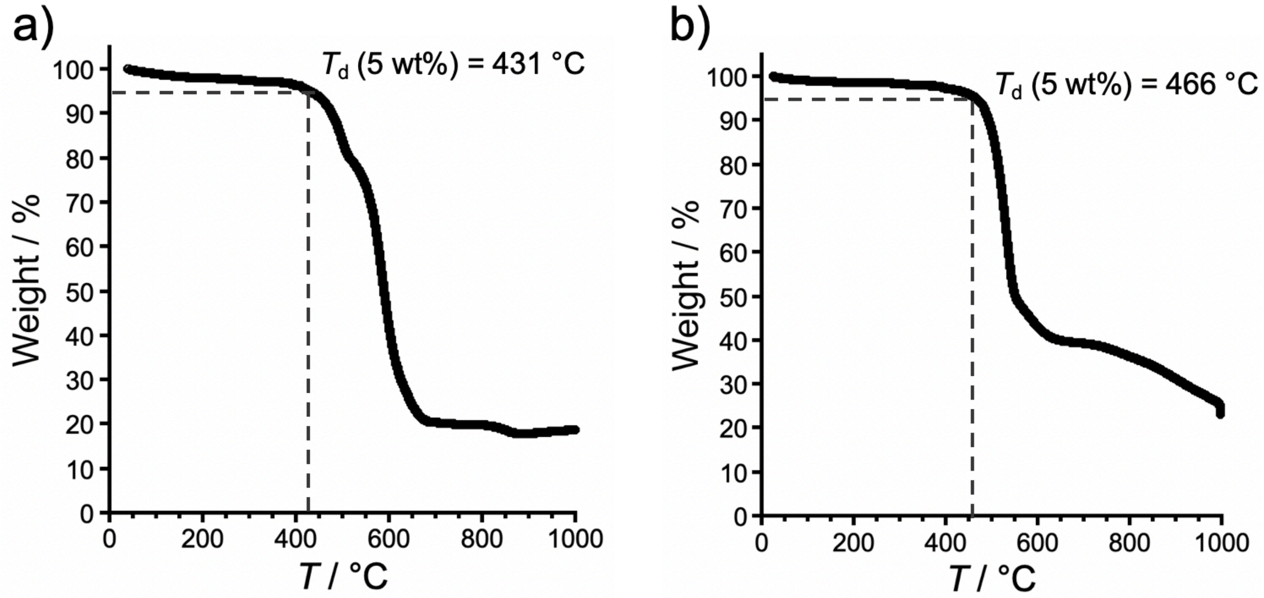

Fig. S2 TGA profiles of **1** under a) air and b) N_2 gas flow.

Copies of NMR Charts.

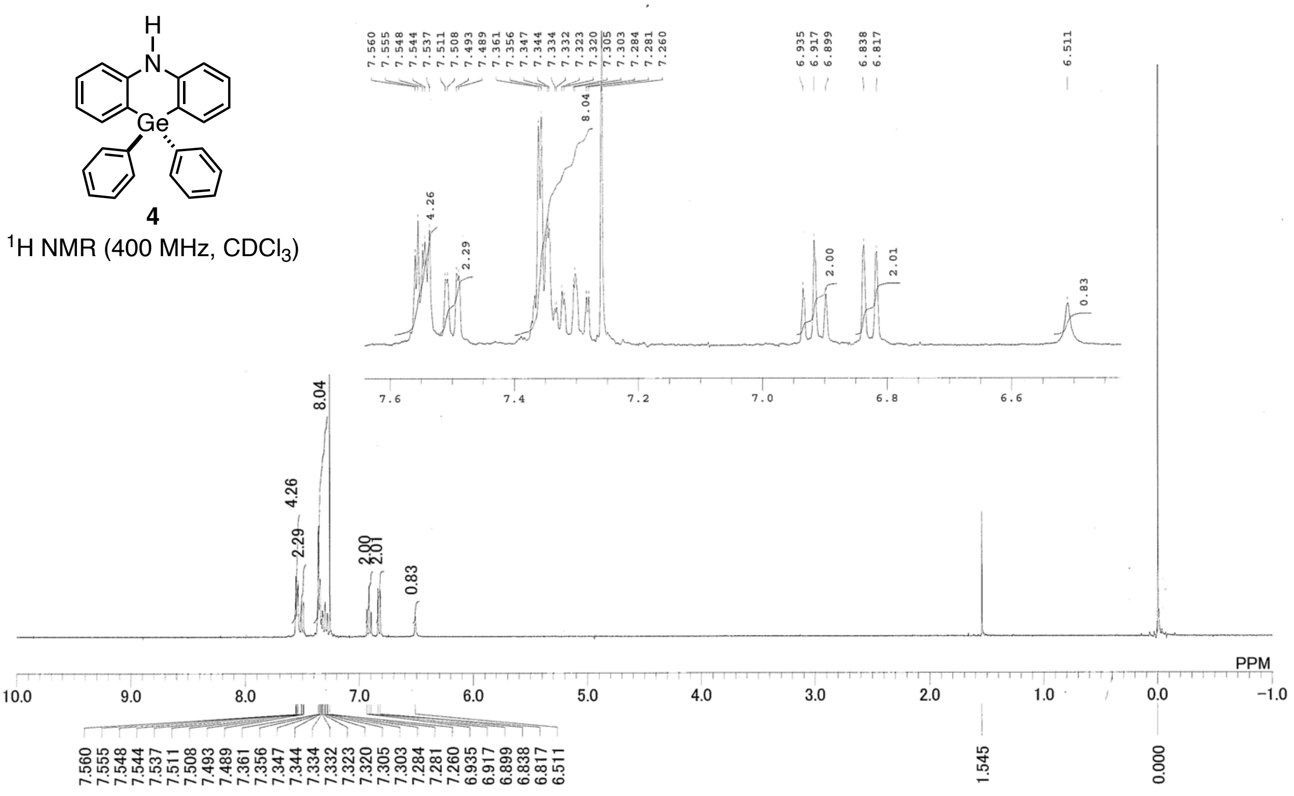

4

^{1}H NMR (400 MHz, CDCl$_3$)

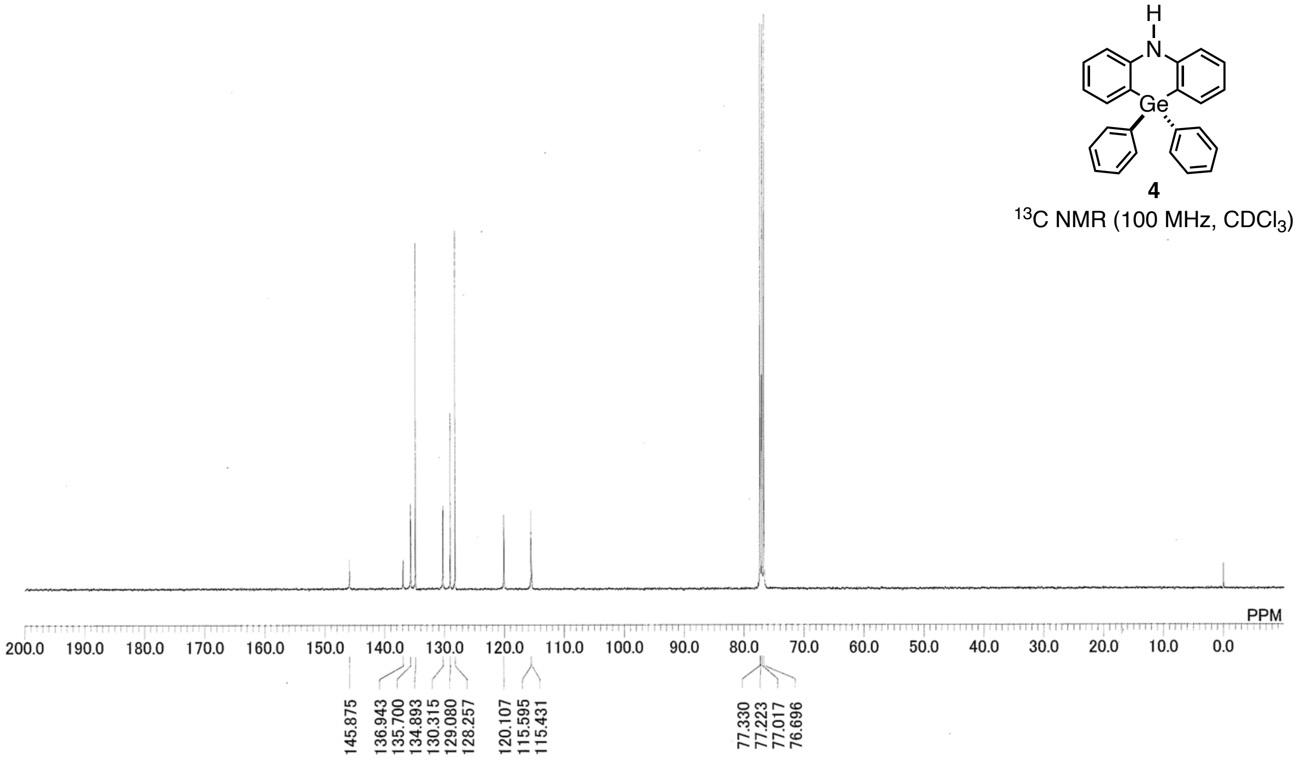

4

^{13}C NMR (100 MHz, CDCl$_3$)

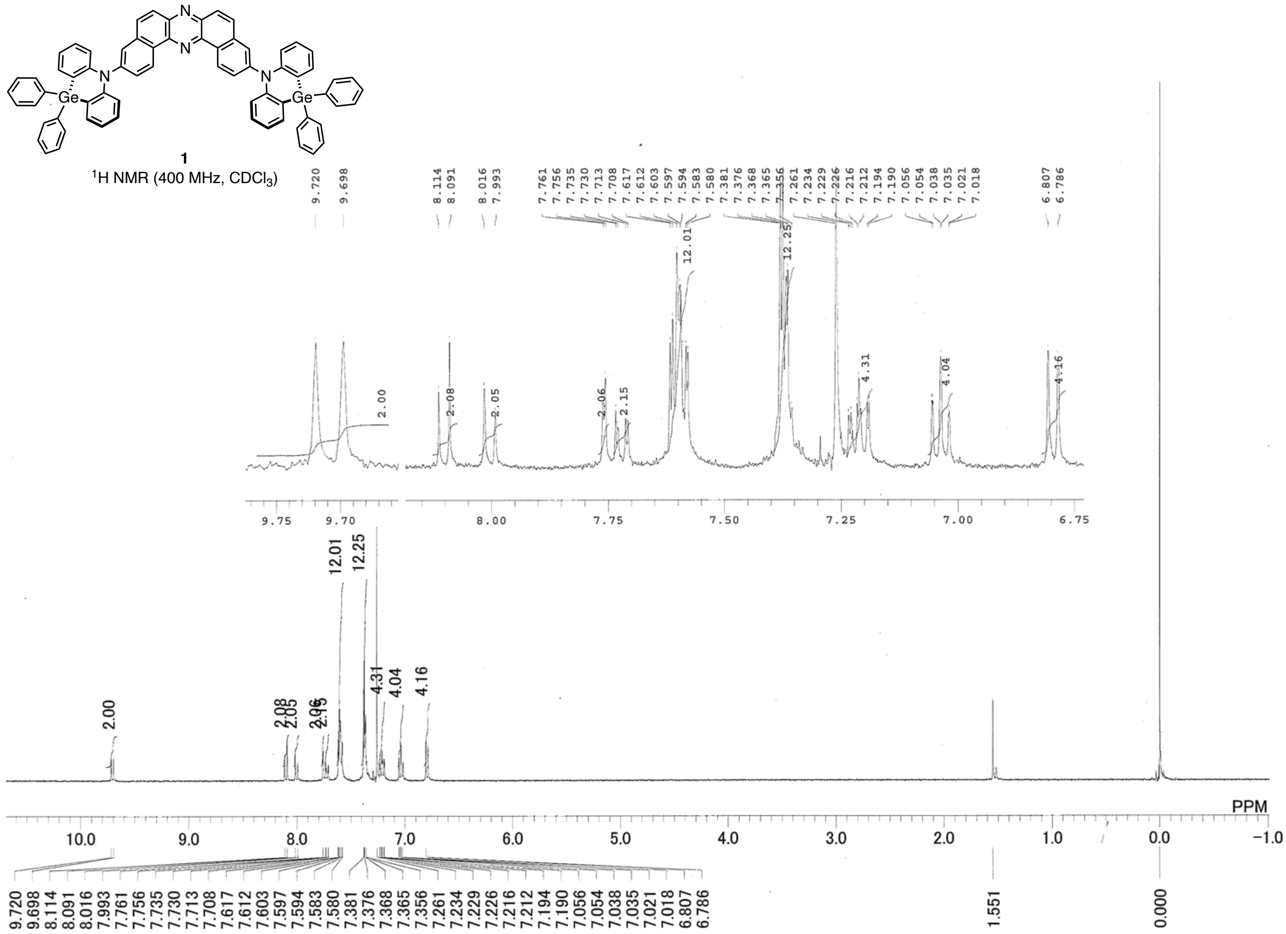

1

^{1}H NMR (400 MHz, CDCl$_3$)

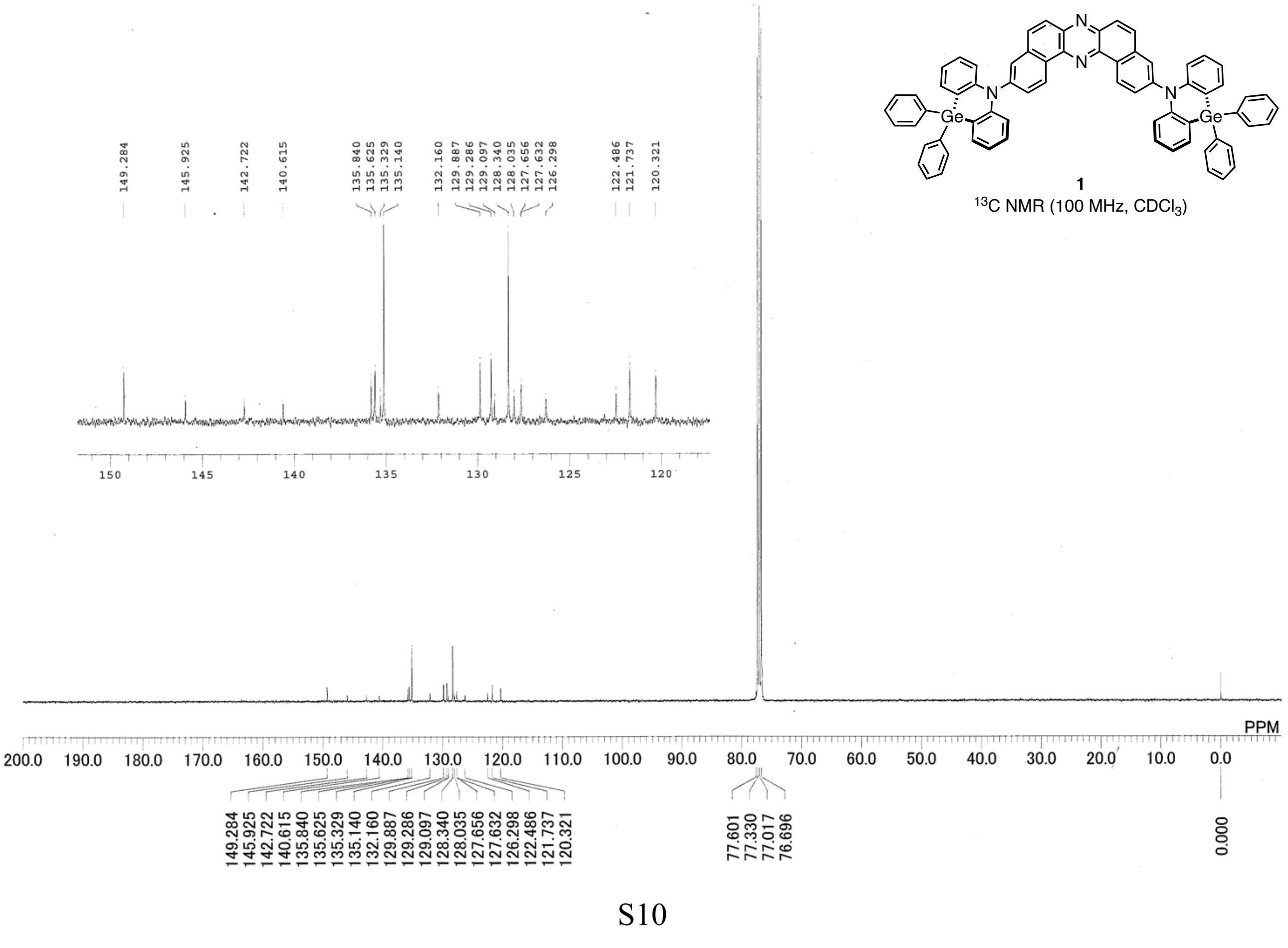

1

^{13}C NMR (100 MHz, CDCl$_3$)

Mataga-Lippert Plot

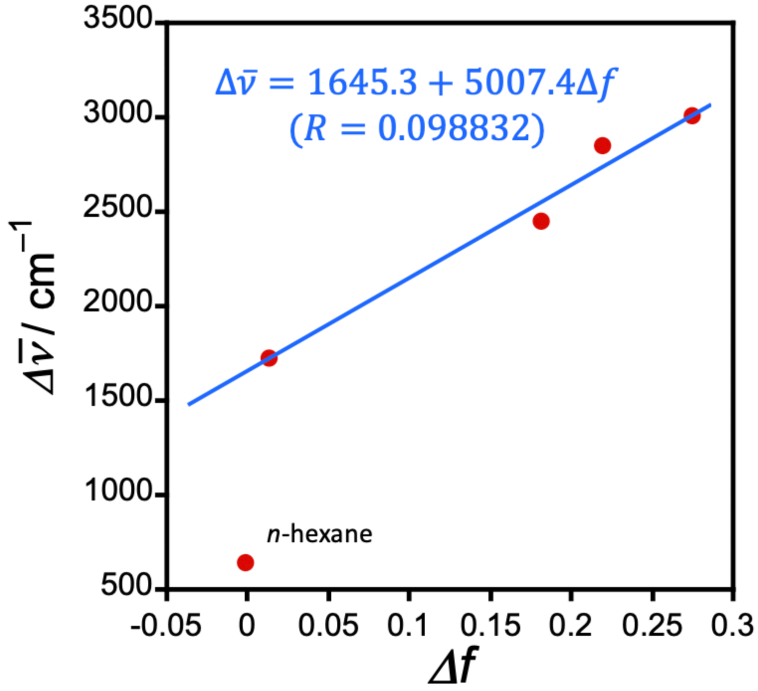

Fig. S3 Mataga-Lippert plot of compound **1**.

Powder X-Ray Diffraction (PXRD) Analysis

Powder X-ray diffraction (PXRD) data were collected on a Rigaku Ultima IV instrument (40 kV, 40 mA) using graphite-monochromateasd CuKα radiation ($\lambda = 1.54187$ Å) at room temperature. The scan rate was 3.0° min^{-1}.

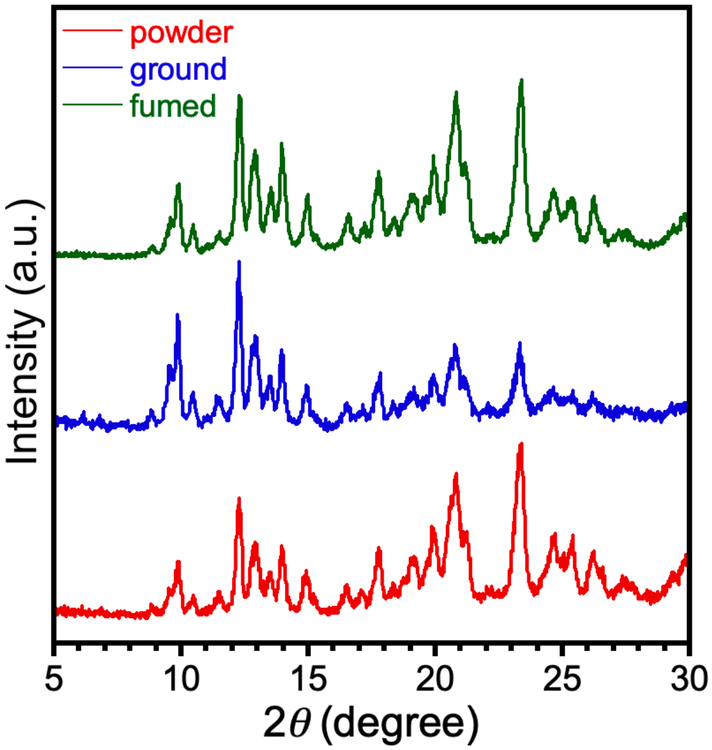

Fig. S4 PXRD patterns of the solid sample **1**.

Theoretical Calculations

Density functional theory (DFT) calculations were performed employing the long-range corrected ωPBE functional along with the 6-31G(d,p) basis set. The functional was non-empirically tuned[S7] resulting in a ω value of 0.167 bohr^{-1}. Excited state calculations applied the Tamm-Dancoff (TDA) approximation[S8] and made use of the polarizable continuum model (PCM) associated with a state specific solvation approach[S9,S10] with toluene as the solvent of choice. The QChem 5.0 package was used throughout.[S11] Fluorescence, phosphorescence and ISC rates were estimated using the nuclear ensemble method[S12], as implemented in the NEMO software interfaced with QChem 5.0. A total of 500 geometries were sampled taking as starting point the optimized geometries of compound **1** at either S_1 or T_1 states. A total of 5 singlet and 5 triplet excited states was calculated for each ensemble.

Table S2 Calculated reorganization energies used in the ISC calculations for singlet to triplet and triplet to singlet transitions**.**

Compound	S -> T (eV)	T -> S (eV)
1	0.054	0.507

Emission Simulations

Table S3 Calculated fluorescence and phosphorescence rates in toluene for compound **1** in the eq-eq conformation.

Process	Rate (s^{-1})	Error (s^{-1})
S_1->S_0	1.2E+07	0.3E+07
T_1->S_0	1.0E+01	0.5E+01
T_2->S_0	2.1E+02	0.8E+02

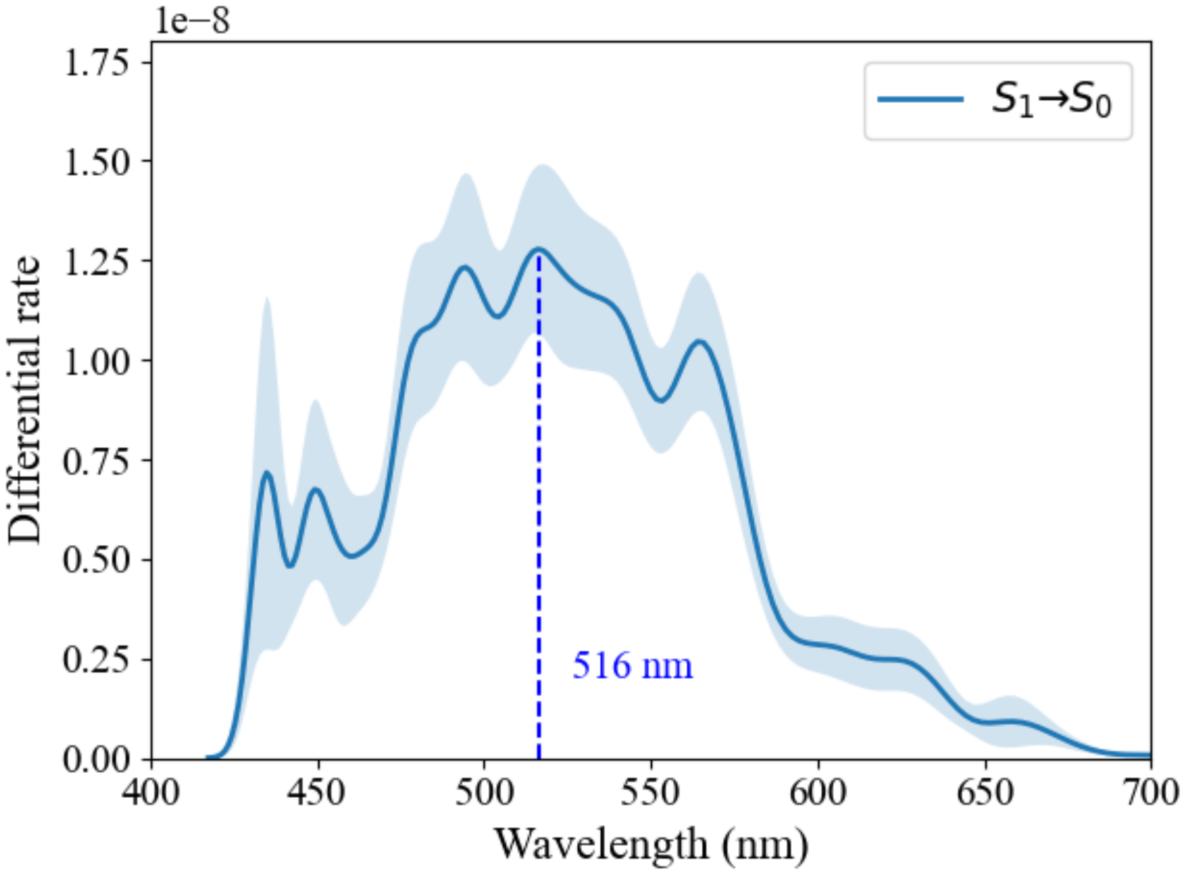

Fig. S5 Simulated fluorescence spectrum for compound **1**. The shadowed region marks the calculated uncertainty.

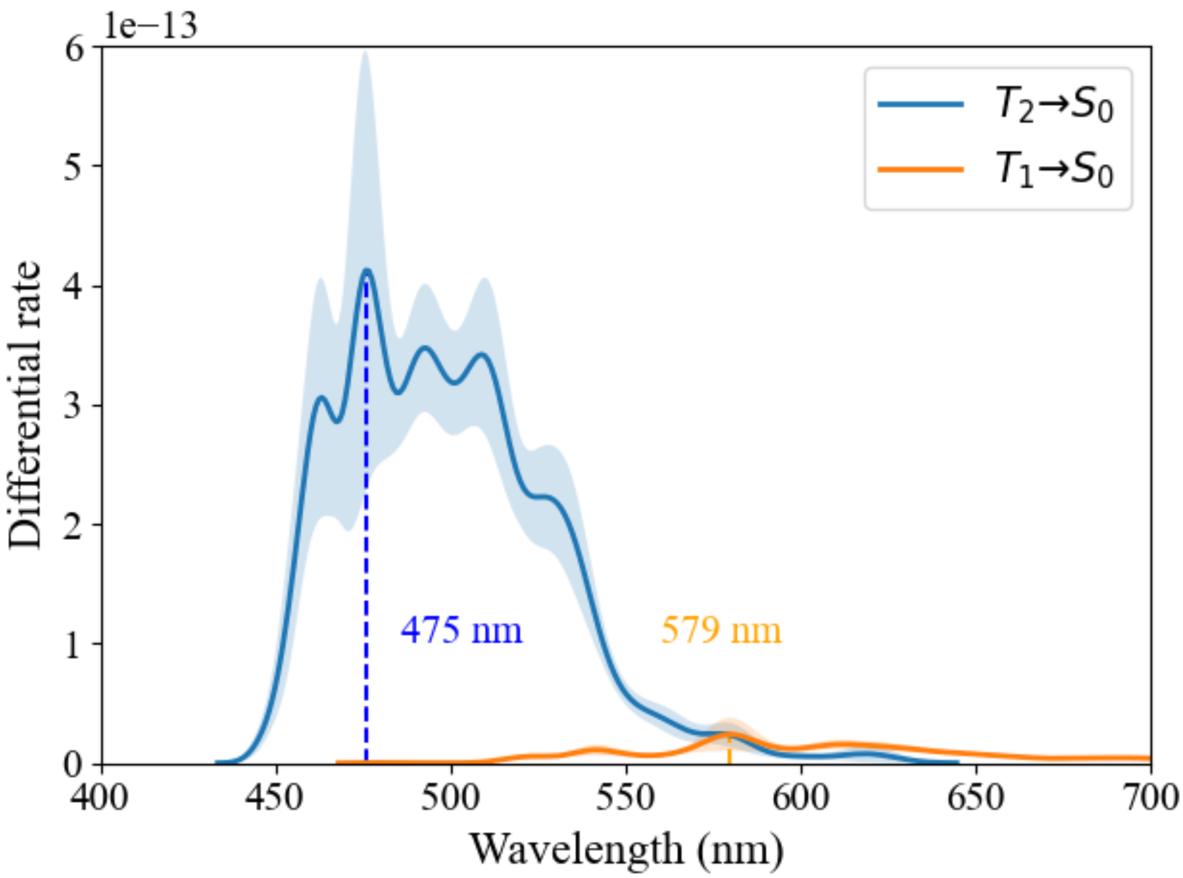

Fig. S6 Simulated phosphorescence spectra for compound **1**. The shadowed region marks the calculated uncertainty.

Intersystem Crossing Rates

Table S4 Estimated ISC rates from the S_1 state for compound **1**.

ISC		
Transfer	Rate (s^{-1})	Error (s^{-1})
S_1->T_1	3.8E+03	3.1E+03
S_1->T_2	9.8E+09	1.6E+09
S_1->T_3	1.1E+09	0.4E+09
S_1->T_4	2.3E+06	1.7E+06
S_1->T_5	3.5E+03	2.6E+03

Table S5 Estimated ISC rates from the T_1 state for compound **1**.

ISC		
Transfer	Rate (s^{-1})	Error (s^{-1})
T_1->S_1	1.8E+01	0.8E+01
T_1->S_2	6.7E-01	6.2E-01
T_1->S_3	3.7E-04	3.0E-04
T_1->S_4	1.1E-06	0.6E-06
T_1->S_5	3.3E-06	3.3E-06

Table S6 Estimated ISC rates from the T_2 state for compound **1**.

ISC		
Transfer	Rate (s^{-1})	Error (s^{-1})
T_2->S_1	2.9E+05	1.7E+05
T_2->S_2	2.7E+04	1.5E+04
T_2->S_3	2.2E+03	1.6E+03
T_2->S_4	4.6E+00	0.9E+00
T_2->S_5	5.6E-02	2.2E-02

Table S7 Average gaps between triplet states for the compound **1**.

Transfer	Average Gap (eV)
T_1->T_2	0.444
T_2->T_3	0.205
T_3->T_4	0.213
T_4->T_5	0.126

Table S8 Estimated probabilities for transfers from the S_1, T_1 and T_2 states for compound **1**.

Transfer	Probability (%)	Transfer	Probability (%)	Transfer	Probability (%)
S_1->T_1	0.0	T_1->S_1	62.5	T_2->S_1	90.6
S_1->T_2	89.5	T_1->S_2	2.3	T_2->S_2	8.7
S_1->T_3	10.4	T_1->S_3	0.0	T_2->S_3	0.7
S_1->T_4	0.0	T_1->S_4	0.0	T_2->S_4	0.0
S_1->T_5	0.0	T_1->S_5	0.0	T_2->S_5	0.0
S_1->S_0	0.1	T_1->S_0	35.2	T_2->S_0	0.1

References

S1 M. Okazaki, Y. Takeda, P. Data, P. Pander, H. Higginbotham, A. P. Monkman and S. Minakata, *Chem. Sci.*, 2017, **8**, 2677–2686.

S2 J. W. Sun, J. Y. Baek, K.-H. Kim, C.-K. Moon, J.-H. Lee, S.-K. Kwon, Y.-H. Kim and J.-J. Kim, *Chem. Mater.*, 2015, **27**, 6675–6681.

S3 Rigaku Oxford Diffraction (2015), Software CrysAlisPro 1.171.39.20a Rigaku Corporation, Tokyo, Japan.

S4 SHELXT Version 2014/5. G. M. Sheldrick, *Acta Cryst.*, 2014, **A70**, C1437.

S5 CrystalStructure 4.2.5: Crystal Structure Analysis Package, Rigaku Corporation (2000-2017). Tokyo 196-8666, Japan.

S6 SHELXL Version 2018/1: G. M. Sheldrick, *Acta Cryst*., 2008, **A64**, 112–122.

S7 T. Stein, L. Kronik and R. Baer, *J. Am. Chem. Soc.,* 2009, **131**, 2818–2820.

S8 S. Hirata and M. Head-Gordon, *Chem. Phys. Lett.*, 1999, **314**, 291–299.

S9 J.-M. Mewes, Z.-Q. You, M. Wormit, T. Kriesche, J. M. Herbert and A. Dreuw, *J. Phy. Chem. A*, 2015, **119**, 5446–5464.

S10 Z.-Q. You, J.-M. Mewes, A. Drew and J. Herbert, *J. Chem. Phys.*, 2015, **143**, 20414.

S11 Y. Shao, Z. Gan, E. Epifanovsky, A. T. B. Gilbert, M. Wormit, J. Kussmann, et al. *Mol. Phys.,* 2015, **113**, 184–215.

S12 L. E. de Sousa, https://github.com/LeonardoESousa/NEMO

Acknowledgement

Y.T. acknowledges a Grant-in-Aid for Scientific Research on Innovative Areas “Aquatic Functional Materials: Creation of New Materials Science for Environment-Friendly and Active Functions” (JSPS KAKENHI Grant Number JP19H05716) from the MEXT, a Grant-in-Aid for Scientific Research (B) (JSPS KAKENHI Grant Number JP20H02813), and a Grant-in-Aid for Challenging Research (Exploratory) (JSPS KAKENHI Grant Number JP21K18960). Y.T. and S.M. acknowledge NIPPOH CHEMICALS for supplying *N,N*-diiodo-5,5-dimethylhydantoin (DIH). P. de S. and L. E. de S. acknowledge support by a research grant (00028053) from VILLUM FONDEN. P.D. acknowledge the support received from the First Team program of the Foundation for Polish Science co-financed by the European Union under the European Regional Development Fund (project number: First TEAM POIR.04.04.00-00-4668/17-00). M.S. acknowledges the support from the Rector of the Silesian University of Technology (BKM-554/RCH4/2021). Y.T., A.N., M.S., P. de S. and P.D. acknowledge the EU’s Horizon 2020 for funding the OCTA project under grant agreement No 778158. Research work supported from the funds for science in 2018-2022 allocated to the implementation of an international co-financed project by the Polish Ministry of Education and Science. P.D., A.N. and M.S. acknowledges the supporting actions from EU’s Horizon 2020 ERA-Chair project ExCEED, grant agreement No 952008. We thank Mr. Takahiro Ami for his assistance of PXRD experiment.